Eur Biophys J (1998) 28: 48–58

ARTICLE

Veronica Beswick · Raphaël Guerois
Françoise Cordier-Ochsenbein · Yves-Marie Coïc
Tam Huynh-Dinh · Jean Tostain · Jean-Pierre Noël
Alain Sanson · Jean-Michel Neumann

Dodecylphosphocholine micelles as a membrane-like environment: new results from NMR relaxation and paramagnetic relaxation enhancement analysis

Received: 16 April 1998 / Revised version: 19 June 1998 / Accepted: 30 July 1998

Abstract To further examine to what extent a dodecylphosphocholine (DPC) micelle mimics a phosphatidylcholine bilayer environment, we performed ^{13}C, ^{2}H, and ^{31}P NMR relaxation measurements. Our data show that the dynamic behavior of DPC phosphocholine groups at low temperature (12 °C) corresponds to that of a phosphatidylcholine interface at high temperature (51 °C). In the presence of helical peptides, a PMP1 fragment, or an annexin fragment, the DPC local dynamics are not affected whereas the DPC aggregation number is increased to match an appropriate area/volume ratio for accommodating the bound peptides. We also show that quantitative measurements of paramagnetic relaxation enhancements induced by small amounts of spin-labeled phospholipids on peptide proton signals provide a meaningful insight on the location of both PMP1 and annexin fragments in DPC micelles. The paramagnetic contributions to the relaxation were extracted from intra-residue cross-peaks of NOESY spectra for both peptides. The location of each peptide in the micelles was found consistent with the corresponding relaxation data. As illustrated by the study of the PMP1 fragment, paramagnetic relaxation data also allow us to supply the missing medium-range NOEs and therefore to complete a standard conformational analysis of peptides in micelles.

V. Beswick · R. Guerois · F. Cordier-Ochsenbein · A. Sanson
J.-M. Neumann (✉)
Département de Biologie Cellulaire et Moléculaire,
Section de Biophysique des Protéines et des Membranes,
URA CNRS 2096, CEA Saclay,
F-91191 Gif sur Yvette Cedex, France

Y.-M. Coïc · T. Huynh-Dinh
Unité de Chimie Organique, URA CNRS 487, Institut Pasteur,
28 Rue du Dr. Roux, F-75724 Paris Cedex 15, France

J. Tostain · J.-P. Noël
Service des Molécules Marquées, CEA Saclay,
F-91191 Gif sur Yvette Cedex, France

A. Sanson
Université P. et M. Curie,
9 Quai Saint-Bernard, Bât. C, F-75005 Paris, France

Key words Dodecylphosphocholine · Peptide-lipid interaction · Paramagnetic probe · NMR

Abbreviations *CI* Chemical ionization · *CPMG* Carr-Purcell-Meiboom-Gill sequence · *DPC* Dodecylphosphocholine · *DQF-COSY* Double quantum filtered correlated spectroscopy · *DPPC* 1,2-dipalmitoyl-*sn*-glycero-3-phosphocholine · *DSS* 2,2-dimethyl-2-silapentane-5-sulfonate · *HPLC* High-pressure liquid chromatography · *JR* "Jump and return" pulse sequence · *MS* Mass spectrometry · *MPLC* Medium-pressure liquid chromatography · *NMR* Nuclear magnetic resonance · *NOE* Nuclear Overhauser effect · *NOESY* Nuclear Overhauser enhancement spectroscopy · *PMP* Plasma membrane proteolipid · *SDS* Sodium dodecyl sulfate · *TFA* Trifluoroacetic acid · *THF* Tetrahydrofuran · *TLC* Thin layer chromatography · *TOCSY* Total correlated spectroscopy

Introduction

Since the pioneering work of Lauterwein et al. (1979), perdeuterated dodecylphosphocholine (DPC) micelles have been widely used as a membrane-like environment for NMR conformational studies of peripheral proteins (Van den Berg et al. 1995; Dauplais et al. 1995), membrane proteins (McDonnell et al. 1993; Papavoine et al. 1995), signal peptides, effector peptides, and more generally protein fragments (Brown and Wüthrich 1981; Wider et al. 1982; Inagaki et al. 1989; Karslake et al. 1990; Malikayil et al. 1992; Constantine et al. 1993; Macquaire et al. 1993; Hammen et al. 1994; Kallick et al. 1995; Segawa et al. 1995; Bechinger 1996; Beswick et al. 1996; Doak et al. 1996; Cowsik et al. 1997; Fletcher and Keire 1997; Fregeau Gallagher et al. 1997; Gesell et al. 1997; MacKenzie et al. 1997; Tessmer and Kallick 1997; Wang et al. 1997; Bechinger et al. 1998; Beswick et al. 1998; Ruan et al. 1998), as well as of lipopeptides (Macquaire et al. 1992; Johansson et al. 1995) or phospholipids (Sanson et al. 1995).

The choice of DPC micelles as a model membrane system arises mainly from the presence of phosphocholine head groups expected to simulate a membrane interface. To further examine to what extent a DPC micelle mimics a phosphatidylcholine environment, we performed ^{13}C, ^{2}H, and ^{31}P NMR relaxation measurements. Protonated DPC and uniformly or selectively deuterated DPC were used for ^{13}C and ^{2}H relaxation experiments, respectively. The dynamic behavior of DPC was compared to those of phospholipids and of two other detergents. Then, the effects on the DPC dynamics resulting from the binding of two protein fragments were investigated.

The first protein fragment, Ac-A-I-I_{20}-A-T-I-I-Y_{25}-R-K-W-Q-A_{30}-R-Q-R-G-L_{35}-Q-R-F-am, comprises the C-terminal cytoplasmic domain and a part of the predicted transmembrane segment of PMP1, a 38-residue regulatory polypeptide associated with the yeast plasma membrane H^+-ATPase (Navarre et al. 1992, 1994). In previous work (Beswick et al. 1998), a NMR conformational study of this 21-residue peptide, solubilized in DPC micelles, showed that the Ala18-Arg33 segment adopts a unique well-defined α helix. Our data also revealed that the helix is partially buried in the hydrophobic core of the micelle and suggested that the helix axis is tilted with respect to the normal at the micelle surface. This orientation allows the location of all the basic side-chains, or at least their extremities, in the polar micelle interface (Beswick et al. 1998). The DPC dynamics in the presence of the PMP1 fragment were explored by measuring the ^{13}C and ^{31}P relaxation rates.

Similar experiments were performed with another peptide spanning the C-helix of the annexin I domain 2. The conformational properties of several annexin I fragments solubilized in DPC micelles have already been studied in our laboratory (Cordier-Ochsenbein et al. 1998 and references therein). The C-helix sequence of domain 2, Ac-A-S-R-T_{30}-N-K-E-I-R_{35}-D-I-N-R-V_{40}-Y-R-E-E-L_{45}-K-R-D-am, has almost the same size as the PMP1 fragment (22 residues instead of 21). As shown by the chemical shift and nuclear Overhauser enhancement (NOE) data, the Asn31-Asp48 segment of the annexin fragment solubilized in DPC micelles at pH 3 forms a regular amphipathic helix.

In a second part, we show that a meaningful insight to the location in DPC micelles of both peptides, the PMP1 and annexin fragments, can be obtained from a quantitative analysis of paramagnetic broadening induced on the peptide proton signals by spin-labeled phospholipids. In general, for most of the published works dealing with micelles, spin-labeled fatty acids were used as paramagnetic probes (Brown and Wütrich 1981; Papavoine et al. 1994, 1995; Jarvet et al. 1997; Ruan et al. 1998) and only qualitative effects were described. However, it has been shown that a fatty acid anchoring to a membrane is strongly pH dependent. At acidic pH, an experimental condition required to minimize the amide proton exchange in NMR experiments, protonated fatty acids exhibit large fluctuations in position along the membrane normal (Sanson et al. 1987). Such behavior certainly occurs for fatty acids solubilized in DPC micelles and severely decreases their efficiency as local probes. Instead of fatty acids, we decided to use a spin-labeled phospholipid commercially available, 1-palmitoyl-2-stearoyl-(10-doxyl)-*sn*-glycero-3-phosphocholine. Previous work showed that phospholipids in small amounts are easily solubilized in DPC micelles and, moreover, adopt a conformation close to the canonical crystallographic structures (Sanson et al. 1995). The chosen spin-labeled phospholipid possesses a phosphocholine group like DPC, allowing its polar head to be located in the DPC micelle interfacial region. Among the various proposed positions of the nitroxide radical in the stearoyl chain, we selected the tenth one (10-doxyl) corresponding approximately to the "center" of the micelle as judged by molecular modeling (data not shown). The differential paramagnetic broadening observed on the carbon signals of DPC in the ^{13}C NMR spectra validated our choice.

Paramagnetic contributions were extracted from intra-residue NH-CαH cross-peaks of NOESY spectra of PMP1 and annexin fragments, recorded in the presence of increasing amounts of spin-labeled phospholipids. The resulting data enabled us to precisely locate the fragments of PMP1 and annexin I domain 2 in DPC micelles. Furthermore, the location of both peptides was shown to be consistent with the relaxation data.

Theoretical background

DPC dynamics

Quantitative analysis of longitudinal (R_1) and transverse (R_2) relaxation rates of DPC nuclei was performed as follows. Expressions of R_1 and R_2 can be written as (Abragam 1961):

1. ^{13}C and ^{31}P relaxations:

$$R_1 = Nd\,[J(\omega_H-\omega_X) + 3J(\omega_X) + 6J(\omega_H+\omega_X)] + c\,\omega_X^2 J(\omega_X)$$

$$R_2 = N\,(d/2)\,[4J\,(0) + J\,(\omega_H-\omega_X) + 3J\,(\omega_X) + 6J\,(\omega_H) + 6J\,(\omega_H+\omega_X)] + (c/6)\,\omega_X^2[4J\,(0)+3J\,(\omega_X)]$$

where ω_H is the ^1H Larmor frequency, ω_X that of ^{13}C or ^{31}P, and $J\,(\omega)$ the reduced spectral density function. In both equations the first term corresponds to the dipolar contribution and the second to the chemical shift anisotropy (CSA). d is equal to $(\gamma_H^2\gamma_X^2h^2/40\pi^2)\,\langle 1/r_{XH}{}^3\rangle^2$ where the γ symbols are the gyromagnetic ratios, r_{XH} the internuclear X-H distance, and N the number of protons bonded to the X nucleus. c is equal to $2\Delta\sigma^2/15$, where $\Delta\sigma$ is the CSA constant. At 125 MHz the CSA contribution to the ^{13}C relaxation of CH_2 and CH_3 groups is negligible, whereas at 202 MHz the ^{31}P relaxation is solely governed by CSA. The C-H distance and the ^{31}P $\Delta\sigma$ constant are respectively equal to 0.108 nm and 165 ppm.

2. ^{2}H relaxation:

$$R_1 = q\,[J(\omega_D) + 4J(2\,\omega_D)]$$

$$R_2 = (q/2)\,[3J(0) + 5J(\omega_D) + 2J(2\,\omega_D)]$$

where ω_D is the ^2H Larmor frequency and q is a constant equal to $(3\pi^2/10)\ \chi^2$, with χ the quadrupolar coupling constant (170 kHz).

According to the well-known simplified formalism of Lipari and Szabo (1982a, b), the expression of $J(\omega)$ can be written as:

$$J(\omega) = [S^2\ \tau_R/(1+\omega^2\ \tau_R^2)] + (1-S^2)\ \tau_L$$

where τ_R is the overall correlation time, τ_L the correlation time characterizing the internal motions, and S the order parameter. The validity of this expression is limited to τ_L values satisfying the two following conditions: $\tau_L \ll \tau_R$ and $\omega^2\ \tau_L^2 \ll 1$. The overall correlation time was estimated using a micelle radius of 2.3 nm (Lauterwein et al. 1979) and the Stokes-Einstein equation

$$\tau_R = \eta\ V/kT$$

where η is the solvent viscosity, V the micelle spherical volume (50 nm^3), and T the absolute temperature. According to this expression, the overall correlation time is found equal to 11 ns and 17 ns at 25 °C and 12 °C, respectively. Values of τ_L and S were directly derived from the R_1 and R_2 data.

Paramagnetic relaxation enhancement of ^1H NMR signals

Quantitative description of paramagnetic relaxation enhancement (R_{2P}) is usually derived from the Solomon-Bloembergen equation (Solomon and Bloembergen 1956):

$$R_{2P} = (K/r_e^6)\ [4J(0) + 3J(\omega_H)]$$

where r_e is the average electron-proton distance, K a constant equal to 1.23×10^{-32} cm^6 s^{-2} for a nitroxide radical (Gillespie and Shortle 1997), and ω_H the proton Larmor frequency. For small objects such as micelles, the relaxation time of the free electron (τ_S) can be neglected (Gillespie and Shortle 1997). As an upper limit, the $J(\omega)$ values were estimated using the correlation times derived from ^{31}P relaxation data.

Materials and methods

DPC synthesis

Dodecylphosphocholine-d_{38} was obtained from commercially available lauric acid-d_{23}, trimethylamine-d_9, and 2-bromoethanol-d_4 (Eurisotop, France) as follows. Dodecanol-d_{25} was synthesized according to the classical route (Warner and Leitch 1965; Stewart and Kates 1989) from lauric acid-d_{23} via its methyl ester which was purified by liquid chromatography on silica gel (elution with hexane/diethyl ether 80/20) and reduced with lithium aluminum hydride-d_4. Dodecanol-d_{25} was purified by liquid chromatography on silica gel (elution with hexane/diethyl ether 50/50); the overall yield for the two steps was 94%. The condensation of dodecanol-d_{25} with diphenyl chlorophosphate afforded, after catalytic hydrogenation on Pt/C (10%), dodecyl-d_{25} phosphoric acid in 80% yield from lauric acid-d_{23} (Brown 1979). The intermediate diphenyl dodecyl-d_{25} phosphate was purified on silica gel (elution with dichloromethane) and dodecyl-d_{25} phosphoric acid was purified by crystallization from petroleum ether; its chemical purity was controlled by thin layer chromatography (TLC) on cellulose with butan-2-ol/methanol/1.5 N ammonia water (100/30/20). Choline-d_{13} bromide was obtained in 81% yield from trimethylamine-d_9 and 2-bromoethanol-d_4 (Brown 1979). The product was purified by crystallization from anhydrous acetone. Choline-d_{13} *p*-toluenesulfonate was synthesized from the bromide salt and *p*-toluenesulfonate silver salt. The product was obtained, after purification by crystallization from warm acetonitrile and diethyl ether, in 97% yield from choline d_{13} bromide. The condensation of choline-d_{13} *p*-toluenesulfonate with dodecyl-d_{25} phosphate in pyridine and trichloroacetonitrile afforded DPC-d_{38} (Sasse 1964; Rosenthal 1966). The final product was purified by liquid chromatography on silica gel (elution with methanol) and on a resin column (Aldrich HB-3A IWT TMD-8) (elution with THF/water 70/30), followed by two crystallizations, first in dry acetone then by dissolution in chloroform and crystallization with dry acetone. The yield for the final step was 82%. DPC-d_{38} was analyzed by high-pressure liquid chromatography (HPLC) on Zorbax SB C18 with methanol/acetone 60/40 + 5% acetic acid (67%)-water + 5% acetic acid (33%); column temperature 35 °C; detection with evaporating light-scattering detector. The purity was better than 99%. There was only one spot on TLC (cellulose and methanol).

The synthesis of DPC-d_{25}, having a protonated head group and a deuterated alkyl chain, was obtained from dodecyl-d_{25} phosphoric acid and unlabeled choline *p*-toluenesulfonate according to the same experimental conditions as above. The overall yield from dodecyl-d_{25} phosphoric acid was 87%. The chemical purity was better than 99%. HPLC analysis was on Zorbax SB C18 with methanol/acetone 60/40 + 5% acetic acid (67%)-water 100 + 5% acetic acid (33%); column temperature 35°C; detection by evaporating light-scattering detector. There was only one spot on TLC (cellulose and methanol). MS-CI/CH_4 *m/e* 377, the isotopic enrichment measured by MS was 96.5%.

Peptide synthesis

The synthesis of the PMP1 fragment has been described elsewhere (Beswick et al. 1998). That of the peptide corresponding to the C-helix of the annexin I domain 2 was performed as follows, using 0.5 mmol of *p*-methylbenzhydrylamine resin (*p*-MBHA). Stepwise elongation was done using the standard double coupling-capping protocols and afforded 2.9 g of peptide resin (yield: 93%, average yield per coupling: 99.6%). Peptide resin (1.5 g; ~0.25 mmol) was subjected to the low-high HF cleavage. The crude peptide (640 mg) was directly purified by medium-pressure

liquid chromatography (MPLC) using a 10–50% linear gradient of acetonitrile in 0.08% aqueous trifluoroacetic acid (TFA) (pH 2) for 60 min at a 25 ml/min flow rate. The purity (>99%) of the peptide was verified on a Nucleosil 5 mm C18 300 Å analytical column, using a 7–40% linear gradient of acetonitrile in 50 mM ammonium acetate (pH 6) for 20 min at a 1 ml/min flow rate (R_t: 11.82 min). Yield: 280 mg (40%). Positive ion electrospray ionization mass spectra: 2802.56±0.10 Da (expected: 2803.10 Da).

NMR experiments

^{2}H, ^{13}C, and ^{31}P longitudinal (R_1) and transverse (R_2) relaxation rates of DPC micelles were measured on a Bruker DRX 500 spectrometer at 77, 125, and 202 MHz, respectively, using standard sequences (inversion recovery for R_1, Carr-Purcell-Meiboom-Gill (CPMG) or Hahn echo for R_2). For all samples, 150 mM of DPC were used. Protonated DPC and uniformly (d_{38}) or selectively (d_{25}) deuterated DPC were used for ^{13}C and ^{2}H relaxation experiments, respectively. Peptide concentration (PMP1 fragment and annexin I domain 2 fragment) was 3 mM. D_2O and H_2O 20 mM phosphate buffers were used for ^{13}C and ^{2}H relaxation experiments, respectively. Deuterated water was purchased from Eurisotop (France).

1-Palmitoyl-2-stearoyl-(10-doxyl)-*sn*-glycero-3-phosphocholine was purchased from Avanti polar lipids (Alabama, USA). Peptide (PMP1 or annexin fragment) and spin-labeled phospholipids were cosolubilized in H_2O/D_2O 9/1 (20 mM phosphate buffer) containing 150 mM of perdeuterated DPC micelles. Four different spin-label (SL) concentrations were used corresponding to relative spin-label to peptide concentration ratios ([SL]/[P]) of 0.0, 0.5, 0.85, and 1.2 (with a peptide concentration of 3 mM). For each peptide, four corresponding NOE spectroscopy (NOESY) phase sensitive spectra with a mixing time of 100 ms were collected using the same experimental conditions on a Bruker DRX 500 spectrometer. The water resonance was suppressed either by presaturation or by using the "jump and return" (JR) sequence (Plateau and Guéron 1982). Thirty two transients were acquired with a recycling delay of 1 s. The temperature was kept at 25 °C and the pH adjusted to 5 (PMP1 fragment) or 3 (annexin fragment).

For the conformational study of the annexin fragment, standard sets of double quantum filtered correlated spectroscopy (DQF-COSY), total correlated spectroscopy (TOCSY), and NOESY experiments were performed on a Bruker DRX 500 spectrometer. The peptide (3 mM) was solubilized in the presence of perdeuterated DPC micelles (150 mM) in H_2O/D_2O (9/1) at pH 3 and a set of NMR experiments was recorded at 25 °C. Without changing the DPC concentration (150 mM), the peptide concentration was decreased tenfold and NMR spectra were recorded. No difference was observed between the spectra corresponding to both peptide concentrations (3 and 0.3 mM), which is in favor of monomeric species. Chemical shifts were referenced from the 2,2-dimethyl-2-silapentane-5-sulfonate (DSS) signal. The water resonance was suppressed either by presaturation or by using the JR sequence. In general, 64 transients were acquired with a recycling delay of 1 s; 400 increments of 2K data points were collected for each two-dimensional (2D) experiment. The mixing times were 72 and 100 ms for the TOCSY and NOESY experiments, respectively.

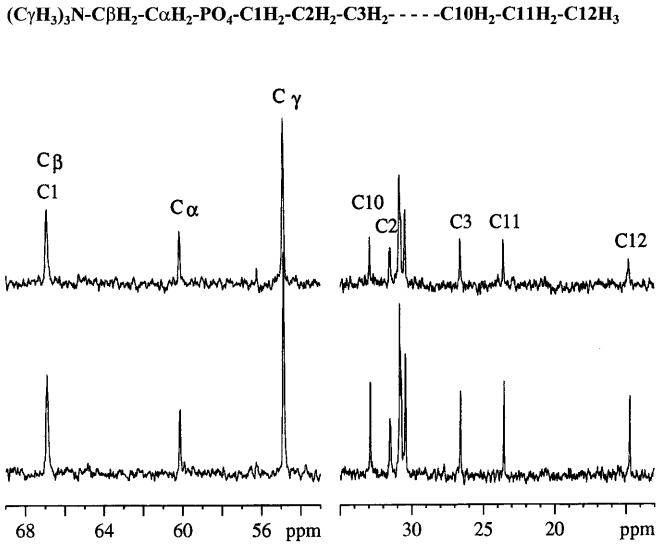

Fig. 1 ^{13}C NMR spectrum of DPC micelles (150 mM, pH 5, 25 °C) in the absence (*bottom*) and presence (*top*) of spin-labeled phospholipids (3 mM). The DPC carbon numbering is indicated

Results and discussion

DPC dynamics in the absence of peptide

As shown in Fig. 1, the ^{13}C spectrum of DPC micelles displays seven well-resolved signals corresponding to the Cγ and Cα head group carbons and to the C2, C3, C10, C11, and C12 chain carbons. The longitudinal and transverse relaxation rates (R_1, R_2) of these nuclei constitute a sufficient data set for characterizing the dynamic behavior of a DPC micelle. The R_1 profile (Fig. 2A) exhibits a plateau region between Cα and C3 with an average value of 2.8±0.1 s^{-1} and a continuous decrease from C10 to C12. The plateau region of the R_2 profile (Fig. 2B) extends from Cα to C10 with an average value of 9.0±1 s^{-1}.

We also performed ^{2}H NMR relaxation measurements on both uniformly (d_{38}-DPC) and selectively (d_{25}-DPC) deuterated micelles. The use of d_{25}-DPC, having a protonated polar head and a deuterated alkyl chain, allowed us to determine the relaxation rates of the C1D$_2$ group of the alkyl chain and those of the CβD$_2$ group whose signals partially overlap in the d_{38}-DPC spectrum. Table 1 lists the R_1 and R_2 values of the resolved deuteron signals. Last, the R_1 and R_2 values of the DPC phosphorus were measured and are reported in Table 2. It is worthwhile noting that, among the three nuclei studied, the DPC ^{31}P exhibits the largest R_2/R_1 ratio (~5 instead of ~3 for ^{13}C and of ~2 for ^{2}H).

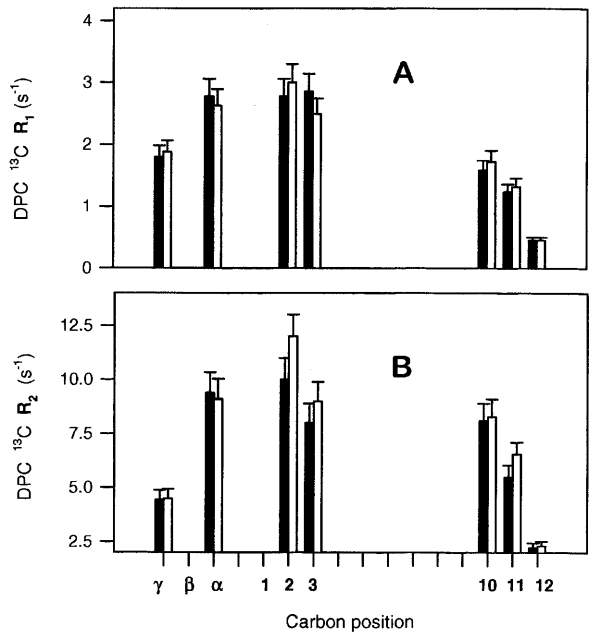

Fig. 2 **A** ^{13}C longitudinal relaxation rate (R_1) of DPC carbons in the absence (*black bars*) and presence (*white bars*) of PMP1 fragment, 12 °C and pH 5; **B** ^{13}C transverse relaxation rate (R_2) of DPC carbons in the absence (*black bars*) and presence (*white bars*) of PMP1 fragment, 12 °C and pH 5

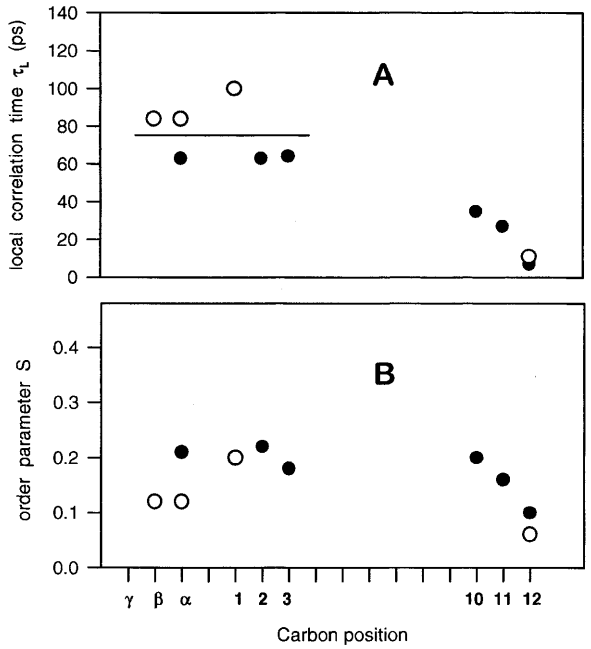

Fig. 3A, B Local correlation time (**A**) and order parameter (**B**) versus DPC carbon position (12 °C, pH 5) deduced from ^{2}H (*open symbols*) and ^{13}C (*filled symbols*) relaxation data

Table 1 Longitudinal (R_1) and transverse (R_2) relaxation rates (in s^{-1}) of DPC deuterons measured at 12 °C and pH 5 (experimental error ± 10%). Longitudinal relaxation rate (in s^{-1}) of DPPC deuterons measured at 51 °C (Seelig and Seelig 1980)

DPC	R_1	R_2	DPPC	R_1
$(C\gamma D_3)_3$	20	20	$(C\gamma D_3)_3$	12
$C\beta D_2$	35	70	$C\beta D_2$	26
$C\alpha D_2$	35	70	$C\alpha D_2$	33
$C1D_2$	50	150	O-CO-$C2D_2$	43
$C12D_3$	5	8	$C16D_3$	4

Table 2 Longitudinal (R_1) and transverse (R_2) relaxation rates (in s^{-1}) of DPC phosphorus (experimental error ± 5%). Estimated apparent volume of DPC micelles (V_A, in nm^3)

Experimental conditions	R_1	R_2	V_A
pH 5 12 °C	1.45	7.75	50
pH 5 12 °C + PMP1 fragment	1.39	9.35	65
pH 3 25 °C	1.20	5.56	50
pH 3 25 °C + annexin fragment	1.26	7.69	80

From the independent sets of ^{13}C and ^{2}H data, values of local correlation times (τ_L) and order parameters (S) at 12 °C were estimated (Fig. 3) as described in Theoretical background. The relaxation data relative to the $(C\gamma H_3)_3$ group were not included in this study since they are insensitive to their environment and reflect only the local rotational motion. Figure 3 shows that the τ_L and S values derived from carbon relaxation data are close to those derived from deuterium relaxation data with, however, several significant differences, especially as regard the head group S values. These discrepancies show the limits of a too simple motion model. In particular, the simplified Lipari-Szabo model does not account for anisotropy effects although it is well known that, in bilayers, the $C\alpha$-$C\beta$-$C\gamma$ head group segment adopts preferential average orientations parallel to the membrane surface. According to molecular simulations (unpublished results), this conformational feature also stands for DPC micelles. Besides, the model does not account for cross-correlation effects. Attempts to obtain a better agreement between our data using a more sophisticated model are out of the scope of this paper and were not undertaken. The τ_L profile exhibits a plateau region extending from the $C\beta$ to the C3 position with an average value of 75 ps. The τ_L value then continuously decreases from the C10 position and reaches 8 ps for the terminal methyl group. The DPC order parameters are found between 0.1 and 0.2 (Fig. 3B). Measurements of DPC relaxation rates recorded at 25 °C give an average τ_L value of 50 ps for the plateau region and 5 ps for the terminal methyl group, without any significant change for the S values.

Dynamic parameters were also derived from the phosphorus R_1 and R_2 data (Table 2). We obtained τ_L values of 250 ps and 200 ps at 12 °C and 25 °C, respectively, with an average S value of 0.25. The τ_L values derived from the phosphorus relaxation data are substantially greater than those obtained from carbon and deuterium relaxation data. In fact, the phosphate group has a larger volume than a CH_2 (CD_2) segment, and its molecular reorientation is therefore slower (Seelig et al. 1981). Furthermore, the phosphate

groups are involved in the hydrogen bond network of interfacial water molecules. In the forthcoming section, we compare the dynamic behavior of DPC to that of other detergents and of phospholipids.

Comparison with other detergents and phospholipids

We first compared the dynamic behavior of the DPC alkyl chains to that of sodium dodecyl sulfate (SDS), another detergent commonly used for NMR studies. Using selectively deuterated SDS and ^{2}H NMR, Söderman et al. (1988a) have estimated the local correlation times of the two first CD_2 groups of the SDS chain and that of the terminal methyl group at 20 °C. τ_L values of 39 ps and 7 ps were respectively obtained for the first groups (average value) and for the terminal group. These values are close to those of the DPC alkyl chains at 25 °C (50 and 5 ps, respectively). Söderman et al. (1988b) have studied the dynamic behavior of another detergent [6-(dimethyleicosylammonio)hexanoate] whose structure is closer to DPC than SDS since it possesses a zwitterionic polar head. ^{14}N NMR relaxation rates were measured for the nitrogen atom connecting the alkyl chain to the polar head, thus having the same position as the phosphorus in DPC. A local correlation time of 175 ps was estimated at 20 °C, a value close to that derived from the DPC ^{31}P relaxation times measured at 25 °C (200 ps).

We then compared our data to those obtained for phospholipids in bilayers. Interestingly, we found that the DPC ^{2}H R_1 values measured at 12 °C are remarkably similar to those of 1,2-dipalmitoyl-*sn*-glycero-3-phosphocholine (DPPC) bilayers obtained at 51 °C and collected by Seelig and Seelig (1980). For comparison, the R_1 values of DPPC deuterons were added in Table 1. Clearly, there is a marked analogy between the local dynamics of the DPC segments at 12 °C and those of DPPC at 51 °C. In particular, one can conclude that the dynamic behavior of the DPC head groups and thus of the DPC interfacial region, at low temperature, is comparable to that of phospholipid interfaces at high temperature. From the relaxation data of DPPC chain deuterons measured at 51 °C, an average τ_L correlation time of 80 ps was estimated for the plateau region (Seelig and Seelig 1980), a value close to that obtained for DPC at 12 °C (75 ps). The DPC order parameters (between 0.1 and 0.2) are also in agreement with the values observed for phospholipid bilayers at high temperature (Seelig and Seelig 1980).

Influence of protein fragments on DPC dynamics

Influence of the PMP1 fragment

Relaxation measurements of DPC phosphorus and carbons in the presence of the PMP1 fragment were performed. As shown in Table 2 and Fig. 2A, the peptide has no influence on the R_1 values of both nuclei. In contrast, the ^{31}P R_2 and some of the ^{13}C R_2 values significantly increase (Fig. 2B, Table 2). It is well known that, in contrast to R_1, R_2 depends on $J(0)$, the spectral density function at zero frequency (see Theoretical background). As a consequence, R_2 is sensitive to variations of both overall and local correlation times whereas R_1 depends mainly on local correlation times. Therefore, our results indicate that: (1) the average local dynamics of a DPC molecule are not affected by the presence of peptide; (2) the presence of peptide leads to an increase of the overall correlation time, i.e., of the apparent volume of DPC micelles. Such an effect has been observed from diffusion coefficient measurements (Kallick et al. 1995). As already indicated by comparing the R_2/R_1 ratios obtained for the various nuclei, the phosphorus relaxation rates are the most sensitive parameters upon variation of the overall correlation time. They also constitute the most accurate data because of the 100% natural abundance and the high gyromagnetic ratio of phosphorus. We thus used the ^{31}P relaxation rates to estimate the increase of the apparent volume of DPC micelles upon peptide binding. Since the R_1 values are insensitive to the presence of peptide, we assumed that the τ_L and S values obtained in the absence of peptide are not modified in their presence. Using these values, an increase from 50 to 65 nm^3 was estimated for the apparent micelle volume (Table 2) after addition of the PMP1 fragment. The increase of the micelle volume, ΔV = 15 nm^3, is greater than the volume of the peptide helix of about 5 nm^3 (from molecular modeling). Since the volume of a DPC molecule is about 1 nm^3, the difference between ΔV and the helix volume corresponds to approximately 10 additional DPC molecules. This means that a reorganization of the micelle occurs in the presence of the peptide, i.e., that the aggregation number is increased to match an appropriate area/volume ratio for accommodating the bound peptide.

Influence of the annexin fragment

Relaxation measurements of DPC phosphorus and carbons in the absence and presence of the annexin fragment at 25 °C and pH 3 were then performed. Under these experimental conditions, the annexin fragment forms a well-defined amphipathic helix bound to DPC micelles (see below). As in the case of the PMP1 fragment, the R_1 values of both nuclei are insensitive to the presence of peptide (Table 2 and Fig. 4A). Therefore, it can be concluded that small peptides such as PMP1 and annexin fragments have no influence on the average local dynamics of DPC molecules at the NMR timescale. The presence of the annexin fragment increases the transverse relaxation rates (Table 2 and Fig. 4B), with a maximum variation of 40% observed for the ^{31}P R_2. Analysis of ^{31}P R_1 and R_2 values indicates that the binding of the annexin fragment leads to an increase of the micelle volume, ΔV, of 30 nm^3 (Table 2), a variation significantly greater than that observed in the case of the PMP1 fragment. The difference between ΔV and the annexin helix volume corresponds approximately to 25 additional DPC molecules.

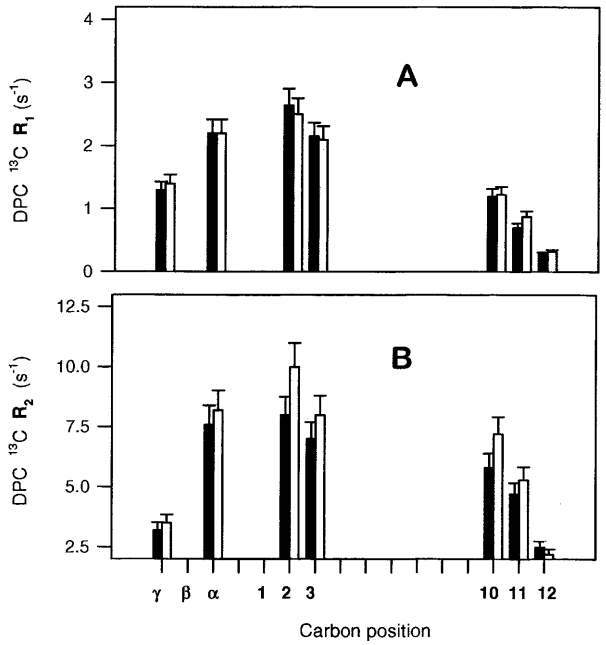

Fig. 4 **A** ^{13}C longitudinal relaxation rate (R_1) of DPC carbons in the absence (*black bars*) and presence (*white bars*) of annexin fragment, 25 °C and pH 3; **B** ^{13}C transverse relaxation rate (R_2) of DPC carbons in the absence (*black bars*) and presence (*white bars*) of PMP1 fragment, 25 °C and pH 3

Location of peptides in DPC micelles using spin-labeled phospholipids

In this section, we show how the location of the PMP1 and annexin fragments within DPC micelles can be precisely determined using spin-labeled phospholipids and how these respective locations can be related to the ^{31}P relaxation data. Figure 1 displays the ^{13}C spectrum of protonated DPC (150 mM) in the absence and presence of 1-palmitoyl-2-stearoyl-(10-doxyl)-*sn*-glycero-3-phosphocholine (3.5 mM). As expected, the spin-labeled phospholipid induces a significant paramagnetic broadening of the alkyl chain carbon signals, more pronounced for those located at the end. The relative linewidth increase is about 40% for the C2 and C3 signals, 50% for C10 and C11, and 60% for C12. On the other hand, the effect of spin-labeled phospholipids on the polar head carbons is substantially reduced (linewidth increases of about 25%). The nitroxide radical is thus on average located near the end of DPC chains, i.e., near the "center" of the micelle. In the presence of peptide (3 mM of PMP1 fragment) the paramagnetic effect on DPC carbons was found to be quite similar.

Location of the PMP1 fragment

To estimate the location of each aminoacid of the PMP1 fragment with respect to the nitroxide radical, we measured the paramagnetic relaxation enhancement induced on each intra-residue (NH-CαH) cross-peak of NOESY spectra. TOCSY spectra were not used since, during the spin-

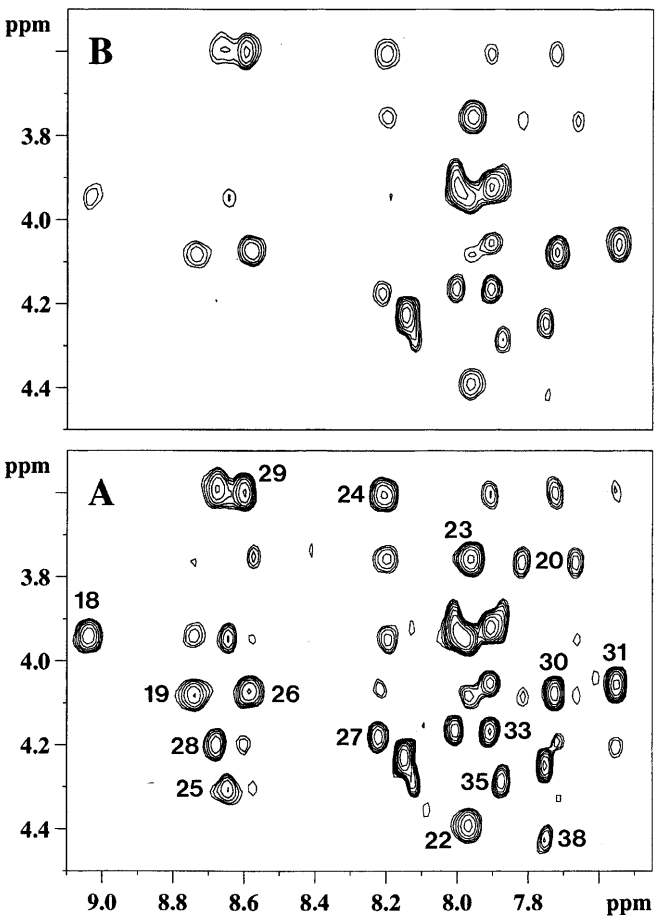

Fig. 5 A, B Part of a NOESY spectrum (500 MHz, 100 ms mixing time, 25 °C, pH 5) of the PMP1 fragment (3 mM) solubilized in DPC micelles (150 mM) showing the NH-CαH correlations in the absence (**A**) and presence (**B**) of spin-labeled phospholipids ([SL]/[P] = 1.2)

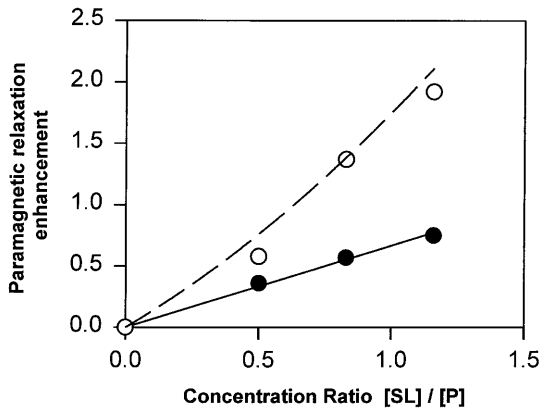

Fig. 6 *Filled symbols*: plot of $(\Delta\nu\,(x) - \Delta\nu_N)/\Delta\nu_N$ versus the relative spin-label concentration (x) obtained from the Ala18 NH linewidth; *dashed line*: plot of $(Y\,(x) - Y_N)/Y_N$ versus the relative spin-label concentration (x) calculated (see text) for the reciprocal volume of the intra-residue NH-CαH cross-peak of Ala18; *open symbols*: experimental plot of $(Y\,(x) - Y_N)/Y_N$ versus the relative spin-label concentration (x) obtained for the reciprocal volume of the intra-residue NH-CαH cross-peak of Ala18

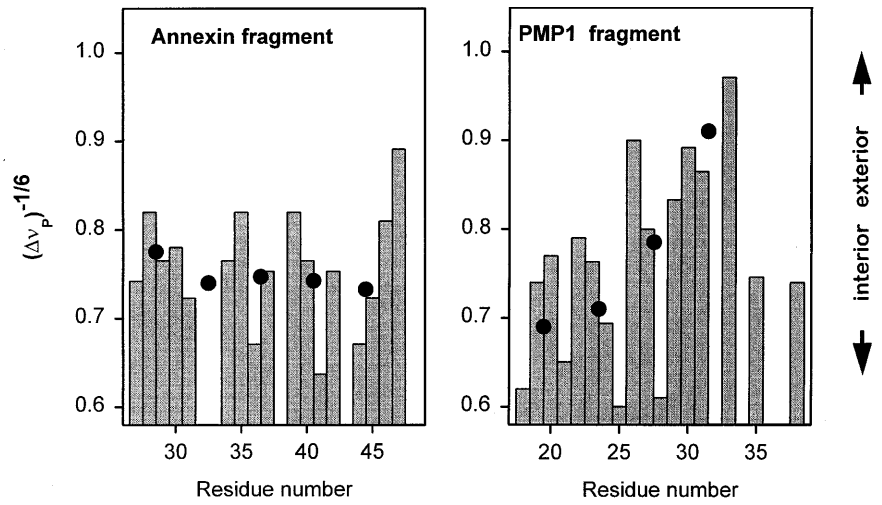

Fig. 7 Plot of $(\Delta\nu_P)^{-1/6}$ (see text) versus residue number obtained at 25 °C for the PMP1 fragment (*right*) and the annexin fragment (*left*) solubilized in DPC micelles. *Filled circles* correspond to the average $(\Delta\nu)^{-1/6}$ values calculated for each group of four consecutive residues of the helix

lock period, significant relaxation of transverse magnetization occurs. NOESY spectra were recorded for three different spin-labeled phospholipid concentrations, corresponding to spin-label to peptide concentration ratios ([SL]/[P]) of 0.5, 0.85, and 1.2. Figure 5 shows the NH-CαH region of a PMP1 fragment NOESY spectrum in the absence (A) and presence (B) of spin-labeled phospholipids ([SL]/[P] = 1.2). All the 16 resolved intra-residue NH-CαH NOE cross-peaks are labeled. One can clearly observe that the paramagnetic broadening is far from being homogeneous and dramatically varies from one residue to another.

A simple method can be used to extract the paramagnetic contribution from the variations of a given intra-residue NOE cross-peak volume on increasing the spin-label concentration. However, this method is based on several approximations which need to be validated. It is thus necessary to first consider the paramagnetic effect on a 1D signal. In the presence of spin-labeled phospholipids, the transverse relaxation rate of a proton of a peptide solubilized in micelles can be expressed as:

$$R_2(x) = R_{2N} + x\,R_{2P}$$

where x is the spin-labeled lipid to peptide concentration ratio ([SL]/[P]), R_{2N} the nuclear transverse self relaxation rate, and R_{2P} the paramagnetic contribution due to electron-nucleus interaction. In the PMP1 fragment NMR spectrum, the Ala18 NH signal is remarkably isolated from the other clustered NH resonances (δ = 9 ppm, Fig. 5). The paramagnetic contribution to its transverse relaxation rate can thus be easily estimated from 1D spectra by measuring the linewidth at half-height:

$$\Delta\nu(x) = R_2(x)/\pi = \Delta\nu_N + x\,\Delta\nu_P$$

Figure 6 shows the plot of $(\Delta\nu(x) - \Delta\nu_N)/\Delta\nu_N$ versus x for the three spin-label concentrations (filled symbols). The corresponding slope gives a value of $\Delta\nu_P/\Delta\nu_N$ (= 0.66).

Let now examine how to extract this ratio from the intra-residue Ala18 NH-CαH NOE cross-peak. In the linear domain (i.e., for short mixing times), the NOE cross-peak signal $S(\omega_1, \omega_2)$ between the NH and CαH protons is of the form (Macura and Ernst 1980):

$$(M_0/4)\,\sigma\,\tau_M\,(R_{2I}/[R_{2I}^2 + (\omega_1-\omega_I)^2])\,(R_{2J}/[R_{2J}^2 + (\omega_2-\omega_J)^2])$$

where M_0, σ, τ_M, ω_I, and ω_J are, respectively, the equilibrium magnetization, the NH-CαH cross-relaxation rate, the NOESY mixing time, the NH and CαH frequencies, and R_{2I} and R_{2J} are the corresponding transverse relaxation rates. The cross-peak volume is obtained by integrating $S(\omega_1, \omega_2)$ on a frequency domain defined by two limits in both dimensions, $(\omega_{11}, \omega_{12})$ in F1 and $(\omega_{21}, \omega_{22})$ in F2. At the first order[1], the cross-peak volume can be expressed as:

$$(M_0/4)\,\sigma\,\tau_M\,(\Delta\omega_1\Delta\omega_2)/(R_{2I}R_{2J}) = M_0\,\sigma\,\tau_M\,(\Delta\nu_1\Delta\nu_2)/(\Delta\nu_I\Delta\nu_J)$$

where $\Delta\omega_1 = \omega_{11} - \omega_{12} = 2\pi\Delta\nu_1$ and $\Delta\omega_2 = \omega_{21} - \omega_{22} = 2\pi\Delta\nu_2$. Since, in general, the NH and CαH protons of a given residue have similar transverse relaxation rates, we may write $\Delta\nu_I \sim \Delta\nu_J \sim \Delta\nu$. Therefore, the intra-residue (NH-CαH) NOE cross-peak volume, V, should be proportional to $1/\Delta\nu^2$. At this step, it is more convenient to consider the reciprocal volume $Y = 1/V$, proportional to $\Delta\nu^2$. In the presence of increasing amounts of spin-labeled phospholipids, it is also reasonable to assume that a similar paramagnetic contribution affects the transverse relaxation rate of the two neighboring Ala18 NH and CαH protons. Given the expression of $\Delta\nu(x)$ mentioned above, the relative variation of Y versus x may therefore be described by the following expression:

$$(Y(x) - Y_N)/Y_N = 2x\,(\Delta\nu_P/\Delta\nu_N) + x^2(\Delta\nu_P/\Delta\nu_N)^2$$

where Y_N and $Y(x)$ are the reciprocal cross-peak volumes in the absence and presence of a relative spin-label con-

[1] The primitive function of $a/(a^2 + u^2)$ is Arctg (u/a), $= u/a$ at the first order

centration x, respectively. This expression may constitute a reasonable approximation providing that a constant integration window is used for measuring the NOE cross-peak volume versus x and that the window dimensions are close to $\Delta\nu_N$ in both frequency domains. Its validity has been tested experimentally as follows.

We calculated the above expression versus the experimental spin-label concentrations using the value of $\Delta\nu_P/\Delta\nu_N$ derived from the 1D Ala18 NH linewidth variations (= 0.66, see above). The resulting plot, shown as a dashed curve in Fig. 6, simulates the expected relative variation of the reciprocal Ala18 (NH,CαH) cross-peak volume on increasing the spin-label concentration, providing that the approximations we made are suitable. Using an appropriate and constant integration window, we measured the experimental $(Y(x) - Y_N)/Y_N$ values corresponding to the Ala18 (NH, CαH) NOE cross-peak for the three different spin-label concentrations (x) (open symbols in Fig. 6). Comparison between the simulated and experimental data is rather satisfactory. Fitting the experimental data, a value of 0.62 was found for $(\Delta\nu_P/\Delta\nu_N)$, close to that measured from the 1D spectra (0.66).

$(Y(x) - Y_N)/Y_N$ ratios relative to all resolved intra-residue (NH-CαH) NOE cross-peaks of the PMP1 fragment were measured for the three spin-label concentrations. For Ala21, the intra-residue Nβ NOE was used. For each amino acid, the corresponding ratios were then fitted to obtain a value of $(\Delta\nu_P/\Delta\nu_N)$. $\Delta\nu_N$ was estimated from a section of the intra-residue cross-peak in the F2 dimension of the NOESY spectrum recorded in the absence of spin-label and a $\Delta\nu_P$ value was obtained from the $(\Delta\nu_P/\Delta\nu_N)$ ratio. Since $\Delta\nu_P$ is proportional to $(r_e)^{-6}$ where r_e is the average electron-nucleus distance (see Theoretical background), we report in Fig. 7 the values of $(\Delta\nu_P)^{-1/6}$, which has also the advantage to minimize the experimental errors. Furthermore, we report in Fig. 7 (filled circles) the average $(\Delta\nu)^{-1/6}$ value calculated for each group of four consecutive residues of the helix. This allows us to average the paramagnetic broadening over residues of a given helix turn and thus to obtain a profile reflecting only the orientation of the helix in the micelle. The distribution of the average values clearly indicates that the helix N-terminus (Ala18) of the PMP1 fragment points toward the nitroxide radical, i.e., toward the "center" of the micelle, while the helix C-terminus (Arg33) points toward the aqueous solution. Interestingly, whereas the lack of medium-range NOEs prevented us from characterizing the conformation of the Gly34-Phe38 C-terminal segment (Beswick et al. 1998), the significant paramagnetic broadening observed for Leu35 and Phe38 (Fig. 7) shows that this segment tends to fold back toward the micelle interior.

Using the quantitative description of $\Delta\nu_P$ reported in Theoretical background, we may locate the helix N- and C-termini (Ala18 and Arg33) respectively at about 1.3 nm and 2.1 nm from the "center" of the micelle. This result provides experimental evidence for our initial suggestion of a tilted helix axis of the PMP1 fragment in DPC micelles (Beswick et al. 1998).

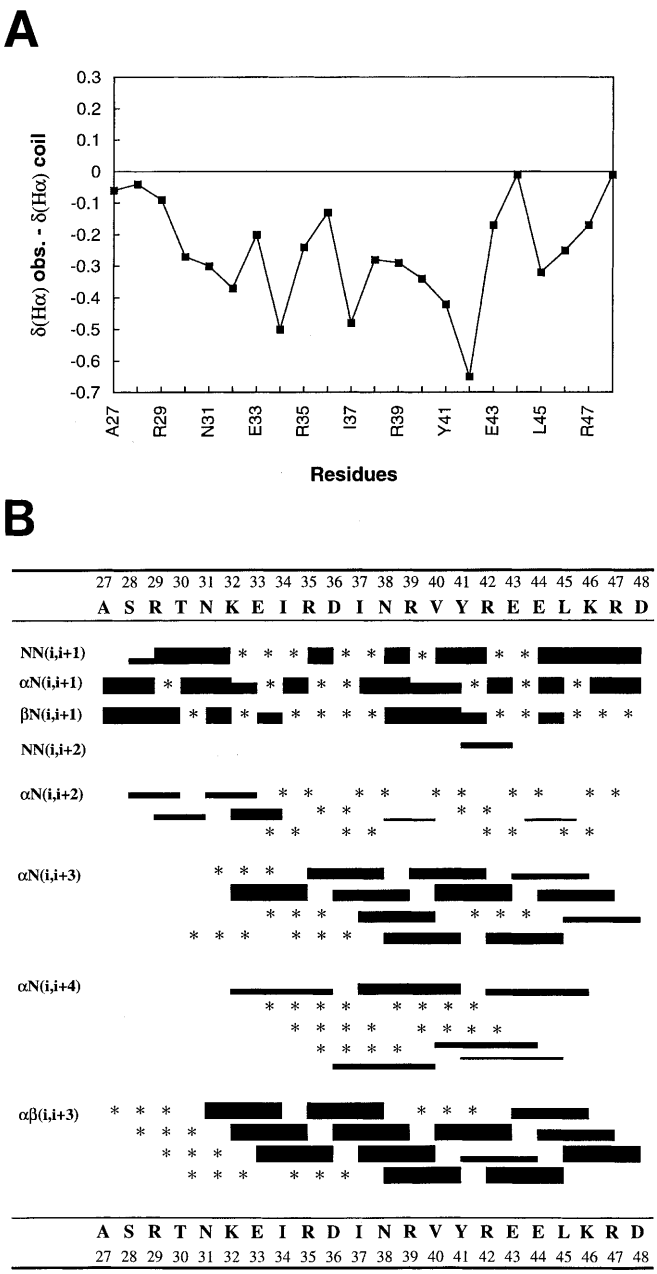

Fig. 8 **A** Hα proton chemical shift indexes, $\Delta\delta H\alpha = \delta H\alpha_{obs} - \delta H\alpha_{coil}$, obtained for the annexin fragment (3 mM) solubilized in DPC micelles (150 mM) at 25 °C and pH 3. The random coil values ($\delta H\alpha_{coil}$) were taken from Merutka et al. (1995). **B** Diagram showing the sequential and medium-range NOE connectivities obtained for the annexin fragment solubilized in the presence of DPC micelles at pH 3 and 25 °C. *Asterisks* refer to ambiguous NOEs

Location of the annexin fragment

Proton assignment and determination of the secondary structure of the peptide corresponding to the C-helix segment of the annexin I domain 2, solubilized in DPC micelles, were straightforward. As shown by the Hα chemical shift indexes (Fig. 8A) and NOE data (Fig. 8B), the Asn31-Asp48 segment adopts a well-defined helix confor-

mation at pH 3, i.e., when the acidic side-chains are protonated.

Using the same experimental conditions as for the PMP1 fragment, NOESY spectra were recorded in the presence of increasing amounts of spin-labeled phospholipids. The resulting $\Delta\nu_P$ values were found more homogeneous than for the PMP1 fragment. Figure 7 shows the $(\Delta\nu_P)^{-1/6}$ histogram and the average value for each group of four consecutive residues. The resulting profile is quite close to that expected for a regular amphipathic helix lying at the interface between the polar medium formed by the hydrated phosphocholine groups and the hydrophobic core formed by the DPC alkyl chains. All the basic residues Arg29, Arg35, Arg39, Arg42, and Lys46 point toward the polar medium (owing to cross-peak overlaps, $\Delta\nu_P$ of Lys32 was not measured).

The respective locations of the PMP1 and annexin fragments in DPC micelles can now be related to the results derived from the ^{31}P relaxation data. These results indicated that the increase of the DPC aggregation number for accommodating a bound peptide is significantly greater for the annexin fragment (25 additional detergent molecules) than for the PMP1 fragment (10 additional detergent molecules). Such a difference can be readily explained by considering that the physical constraints imposed on a spherical micelle for accommodating a helix lying at the interface (annexin fragment) are greater than those relative to a helix partially buried in the hydrophobic core (PMP1 fragment).

Conclusion

Multi-nuclear relaxation measurements provided new experimental evidence showing that DPC micelles constitute a realistic model of membrane interfaces. We showed that they also constitute an appropriate system for obtaining a meaningful insight into peptide location at the interface by combining the measurement of paramagnetic relaxation enhancements according to the method reported in this paper and ^{31}P relaxation data. Furthermore, as illustrated by the study of the PMP1 fragment, paramagnetic relaxation data allow us to supply the missing medium-range NOEs and therefore to complete a standard conformational analysis of peptides in micelles. Nevertheless, it has to be kept in mind that the high curvature of DPC micelles may restrict their use to relatively small peptides or proteins.

Acknowledgements We thank Dr. H. Desvaux, DSM/DRECAM/SCM CEA Saclay, for stimulating discussions about paramagnetic relaxation enhancement in NOESY spectra.

References

Abragam A (1961) The principles of nuclear magnetism. Clarendon, Oxford

Bechinger B (1996) Towards membrane protein design: pH-sensitive topology of histidine-containing polypeptides. J Mol Biol 263: 768–775

Bechinger B, Zasloff M, Opella SJ (1998) Structure and dynamics of the antibiotic peptide PGLa in membranes by solution and solid-state NMR spectroscopy. Biophys J 74: 981–987

Beswick V, Baleux F, Huynh-Dinh T, Képès F, Neumann JM, Sanson A (1996) NMR conformational study of the cytoplasmic domain of the canine Sec61γ protein from the protein translocation pore of the endoplasmic reticulum membrane. Biochemistry 35: 14717–14724

Beswick V, Roux M, Navarre C, Coïc YM, Huynh-Dinh T, Goffeau A, Sanson A, Neumann JM (1998) ^{1}H and ^{2}H-NMR studies of a fragment of PMP1, a regulatory subunit associated with the yeast plasma membrane H^{+}-ATPase; conformational properties and lipid-peptide interactions. Biochimie 80: 451–459

Brown LR (1979) Use of fully deuterated micelles for conformational studies of membrane proteins by high resolution ^{1}H-NMR. Biochim Biophys Acta 557: 135–148

Brown LR, Wüthrich K (1981) Location and orientation relative to the micelle surface for glucagon in mixed micelles with dodecylphosphocholine. Biochim Biophys Acta 647: 95–111

Constantine KL, Mapelli C, Meyers CA, Friedrichs MS, Krystek S, Mueller L (1993) Micelle-bound conformational preferences of a peptide derived from a murine major histocompatibility complex class I molecule. J Biol Chem 268: 22830–22837

Cordier-Ochsenbein F, Guerois R, Baleux F, Huynh-Dinh T, Lirsac PN, Russo-Marie F, Neumann JM, Sanson A (1998) Exploring the folding pathways of annexin I, a multi-domain protein. I. Nonnative structures stabilize the partially folded state of the isolated domain 2 of annexin I. J Mol Biol 279: 1163–1175

Cowsik SM, Lücke C, Rüterjans H (1997) Lipid-induced conformation of substance P. J Biomol Struct Dyn 15: 27–36

Dauplais M, Neumann JM, Pinkasfeld S, Menez A, Roumestand C (1995) Interaction of cardiotoxin γ from *Naja nigrocollis* with perdeuterated dodecylphosphocholine micelles. A proton NMR study. Eur J Biochem 230: 213–220

Doak DG, Mulvey D, Kawaguchi K, Villalain J, Campbell ID (1996) Structural studies of synthetic peptides dissected from the voltage-gated sodium channel. J Mol Biol 258: 672–687

Fletcher TG, Keire DA (1997) The interaction of beta-amyloid protein fragment (12–28) with lipid environments. Protein Sci 6: 666–675

Fregeau Gallagher NL, Sailer M, Niemczura WP, Nakashima TT, Stiles ME, Vederas JC (1997) Three-dimensional structure of leucocin A in trifluoroethanol and dodecylphosphocholine micelles: spatial location of residues critical for biological activity in type IIA bacteriocins from lactic acid bacteria. Biochemistry 36: 15062–15072

Gesell J, Zasloff M, Opella SJ (1997) Two-dimensional ^{1}H NMR experiments show that the 23-residue antibiotic peptide magainin is an alpha-helix in dodecylphosphocholine micelles, sodium dodecylsulfate micelles and trifluoroethanol/water solution. J Biomol NMR 9: 127–135

Gillespie JR, Shortle D (1997) Characterization of long-range structure in the denatured state of staphylococcal nuclease. I. Paramagnetic relaxation enhancement by nitroxide spin labels. J Mol Biol 268: 158–169

Hammen PK, Gorenstein DG, Weiner H (1994) Structure of the signal sequences for two mitochondrial matrix proteins that are not proteolytically processed upon import. Biochemistry 33: 8610–8617

Inagaki F, Shimada I, Kawaguchi K, Hirano M, Terasawa I, Ikura T, Go N (1989) Structure of melittin bound to perdeuterated dodecylphosphocholine micelles as studied by two-dimensional NMR and distance geometry calculations. Biochemistry 28: 5985–5991

Jarvet J, Zdunek J, Damberg P, Gräslund A (1997) Three-dimensional structure and position of porcine motilin in sodium dodecylsulfate. Biochemistry 36: 8153–8163

Johansson J, Szyperski T, Wüthrich K (1995) Pulmonary surfactant-associated polypeptide SP-C in lipid micelles: CD studies of intact SP-C and NMR secondary structure determination of dipalmitoyl-SP-C(1-17). FEBS Lett 362: 261–265

Kallick DA, Tessmer MR, Watts CR, Li CY (1995) The use of dodecylphosphocholine micelles in solution NMR. J Magn Reson B 109: 60–65

Karslake C, Piotto ME, Pak YK, Weiner H, Gorenstein DG (1990) 2D NMR and structural model for a mitochondrial signal peptide bound to a micelle. Biochemistry 29: 9872–9878

Lauterwein J, Bösch C, Brown LR, Wüthrich K (1979) Physicochemical studies of the protein-lipid interactions in melittin-containing micelles. Biochim Biophys Acta 556: 244–264

Lipari G, Szabo A (1982a) Model-free approach to the interpretation of NMR relaxation in macromolecules. 1. Theory and range of validity. J Am Chem Soc 104: 4546–4558

Lipari G, Szabo A (1982b) Model-free approach to the interpretation of NMR relaxation in macromolecules. 2. Analysis of experimental results. J Am Chem Soc 104: 4559–4570

McDonnell PA, Shon K, Kim Y, Opella SJ (1993) Fd coat protein structure in membrane environments. J Mol Biol 233: 447–463

MacKenzie KR, Prestegard JH, Engelman DM (1997) A transmembrane helix dimer: structure and implications. Science 276: 131–133

Macquaire F, Baleux F, Giaccobi E, Huynh-Dinh T, Neumann JM, Sanson A (1992) Peptide secondary structure induced by a micellar phospholipidic interface: ^{1}H-NMR conformational study of a lipopeptide. Biochemistry 31: 2576–2582

Macquaire F, Baleux F, Huynh-Dinh T, Rouge D, Neumann JM, Sanson A (1993) ^{1}H-NMR conformational study of an annexin I fragment: influence of a phospholipidic micellar environment. Biochemistry 32: 7244–7254

Macura S, Ernst RR (1980) Elucidation of cross relaxation in liquids by two-dimensional NMR spectroscopy. Mol Phys 41: 95–117

Malikayil JA, Edwards JV, McLean LR (1992) Micelle-bound conformations of a bombesin/gastrin releasing peptide receptor agonist and an antagonist by two-dimensional NMR and restrained molecular dynamics. Biochemistry 31: 7043–7049

Merutka G, Dyson HJ, Wright PE (1995) Random coil ^{1}H chemical shifts obtained as a function of temperature and trifluoroethanol concentration for the peptide series GGXGG. J Biomol NMR 5: 14–24

Navarre C, Ghislain M, Leterme S, Ferroud C, Dufour JP, Goffeau A (1992) Purification and complete sequence of a small proteolipid associated with the plasma membrane H^+-ATPase of *Saccharomyces cerevisiae*. J Biol Chem 267: 6425–6428

Navarre C, Catty P, Leterme S, Dietrich F, Goffeau A (1994) Two distinct genes encode small isoproteolipids affecting plasma membrane H^+-ATPase activity of *Saccharomyces cerevisiae*. J Biol Chem 269: 21262–21268

Papavoine CHM, Konings RNH, Hilbers CW, Van de Ven FJM (1994) Location of M13 coat protein in sodium doedecylsulfate micelles as determined by NMR. Biochemistry 33: 12990–12997

Papavoine CHM, Aelen JMA, Konings RNH, Hilbers CW, Van de Ven FJM (1995) NMR studies of the major coat protein of bacteriophage M13. Structural informations of gVIIIp in dodecylphosphocholine micelles. Eur J Biochem 232: 490–500

Plateau P, Guéron M (1982) Exchangeable proton NMR without base-line distorsion, using new strong-pulse sequences. J Am Chem Soc 104: 7310–7311

Rosenthal AF (1966) New, partially hydrolyzable synthetic analogues of lecithin, phosphatidyl ethanolamine, and phosphatidic acid. J Lipid Res 7: 779–785

Ruan KH, Li D, Ji J, Lin YZ, Gao X (1998) Structural characterization and topology of the second potential membrane anchor region in the thromboxane A2 synthase amino-terminal domain. Biochemistry 37: 822–830

Sanson A, Egret-Charlier M, Bouloussa O, Maget-Dana R, Charles M, Ptak M (1987) N-acylaminoacids: amphiphilic properties and interactions with the lipid bilayers. In: Mittal KL, Bothorel P (eds) Surfactants in solution, vol 5. Plenum Press, New York, pp 793–805

Sanson A, Monck MA, Neumann JM (1995) Two-dimensional ^{1}H-NMR conformational study of phosphatidylserine diluted in perdeuterated dodecylphosphocholine micelles. Evidence for a pH induced conformational transition. Biochemistry 34: 5938–5944

Sasse K (1964) Organische phosphor-verbindungen. In: Müller E (ed) Methoden der Organischen Chemie (Houben-Weyl), vol. 12. Thieme, Stuttgart, p 232

Seelig A, Seelig J (1980) Lipid conformation in model membranes and biological membranes. Q Rev Biophys 13: 19–61

Seelig J, Tamm L, Hymel L, Fleischer S (1981) Deuterium and phosphorus NMR and fluorescence depolarization studies of functional reconstituted sarcoplasmic reticulum membrane vesicles. Biochemistry 20: 3922–3932

Segawa M, Ohno Y, Doi M, Ishida T, Iwashita T (1995) Solution conformation of μ-selective dermorphin and δ-selective deltorphin-I in phospholipid micelles, studied by NMR spectroscopy and molecular dynamics simulation. Int J Pept Protein Res 46: 37–46

Söderman O, Carlström G, Monduzzi M, Olsson U (1988a) NMR relaxation in micelles. Deuterium relaxation at three field strengths of three positions on the alkyl chain of sodium dodecylsulfate. J Chem Soc Faraday Trans 1 84: 4475–4486

Söderman O, Carlström G, Olsson U, Wong TC (1988b) NMR relaxation in micelles formed by a long zwitterionic surfactant. Langmuir 4: 1039–1044

Solomon I, Bloembergen N (1956) Nuclear magnetic interactions in the HF molecule. J Chem Phys 25: 261–266

Stewart LC, Kates M (1989) Synthesis and characterization of deuterium-labelled dihexadecylglycerol and diphytanylglycerol phospholipids. Chem Phys Lipids 50: 23–42

Tessmer MR, Kallick DA (1997) NMR and structural model of dynorphin A (1–17) bound to dodecylphosphocholine micelles. Biochemistry 36: 1971–1981

Van den Berg B, Tessari M, Boelens R, Dijkman R, Haas GH de, Kaptein R, Verheij HM (1995) NMR structures of phospholipase A_2 reveal conformation changes during interfacial activation. Nat Struct Biol 2: 402–406

Wang G, Sparrow JT, Cushley RJ (1997) The helix-hinge-helix structural motif in human apolipoprotein A-I determined by NMR spectroscopy. Biochemistry 36: 13657–13666

Warner RM, Leitch LC (1965) Deuterated organic compounds XXV. Synthesis of certain deuterated n-Undecanes and n-Dodecanes. J Labelled Compd 1: 42–53

Wider G, Lee KH, Wüthrich K (1982) Sequential resonance assignments in protein ^{1}H-NMR spectra. Glucagon bound to perdeuterated dodecylphosphocholine micelles. J Mol Biol 155: 367–388